Molecular Therapy
Nucleic Acids
Original Article

Circular RNA circCUL3 Accelerates the Warburg Effect Progression of Gastric Cancer through Regulating the STAT3/HK2 Axis

Zhichen Pu,[1,5] Maodi Xu,[1,5] Xiaolong Yuan,[2,3,5] Haitang Xie,[1] and Jun Zhao[4]

[1]Department of Drug Clinical Evaluation Center, Yijishan Hospital of Wannan Medical College, Wuhu, Anhui 241001, China; [2]Department of Pharmacy, Second Affiliated Hospital of Wannan Medical College, Wuhu, Anhui 241001, China; [3]Vascular Diseases Research Center of Wannan Medical College, Wuhu, Anhui 241001, China; [4]Department of Gastrointestinal Surgery, Yijishan Hospital of Wannan Medical College, Wuhu, Anhui 241001, China

The Warburg effect is a significant hallmark of gastric cancer (GC), and increasing evidence emphasizes the crucial role of circular RNAs (circRNAs) in GC tumorigenesis. However, the precise molecular mechanisms by which circRNAs drive the GC Warburg effect are still elusive. The present study was designed to unveil the roles of circRNAs and the corresponding potential mechanism. High-regulated expression of circCUL3 was observed in both GC tissues and cell lines. Clinically, the high expression of circCUL3 was closely correlated with advanced clinical stage and overall survival in GC patients. Functionally, cellular experimental investigations demonstrated that circCUL3 promoted the proliferation, glucose consumption, lactate production, ATP quantity, and extracellular acidification rate (ECAR) of GC cells. *In vivo*, circCUL3 knockdown repressed tumor growth. Mechanistic analysis demonstrated that circCUL3 promoted signal transducer and activator of transcription (STAT)3 expression through sponging miR-515-5p; moreover, transcription factor STAT3 accelerated the transcriptional level of hexokinase 2 (HK2). In summary, the present findings provide mechanistic insights into circCUL3/miR-515-5p/STAT3/HK2 axis regulation on the GC Warburg effect, providing a novel possibility for an understanding of GC pathogenesis.

INTRODUCTION

Gastric cancer (GC) is one of the commonest malignancies and causes of tumor-related deaths worldwide, which has emerged as incisive public health issues characterized with an unfavorable curative effect and poor prognosis.[1,2] Because of the increasing morbidity and mortality, GC brings about great difficulties for patients and a low 5-year survival rate.[3,4] Although multiple methods have been applied for GC, including surgery, chemotherapy, and radiotherapy, the prognosis of patients with GC remains largely unsatisfactory.[5] Increasing evidence has demonstrated the complex etiology for GC tumorigenesis.[6] Hence, elucidating the biologic characteristics and molecular mechanism may be beneficial for the GC treatment.

With the development of high-throughput sequencing, the roles of circular RNA (circRNA) have been adequately identified in GC.[7,8] circRNAs are generated from precursor mRNAs (pre-mRNAs) through back-splicing. Evidence has revealed the biogenesis of circRNAs in eukaryocytes, including splicing factor, eukaryotic initiation factor, and N^6-methyladenosine (m^6A).[9–13] Abundant circRNAs are ubiquitous in eukaryotes, and circRNAs have recently been identified as a new class of regulatory RNAs with genes, including cellular development, neural differentiation, energy metabolism, and occurrence. Being benefited by the covalently closed loop, circRNAs are naturally resistant to exonuclease degradation. Therefore, circRNAs are capable of continuous regulation for tumorigenesis. For example, circCCDC9 expression is downregulated in both GC tissues and cell lines, and mechanistic analysis demonstrated that circCCDC9 acted as a miR-6792-3p sponge to relieve its target, CAV1.[14]

Energy metabolism reprogramming is a remarkable hallmark caused by genomic abnormity.[15–17] The Warburg effect, also known as glycolysis, acts as a significant pathological process in the human cancer.[18] Tumor cells acquire the energy through the Warburg effect to sustain tumor development, including GC. Studies have explicated that the Warburg effect functions as an essential oncogene in GC, and circRNAs could significantly regulate this progression. For example, circNRIP1 acts as a tumor promotor to promote the proliferation, migration, and invasion of GC cells through sponging miR-149-5p to affect the AKT1 expression level in GC.[19] Therefore, it is of pivotal importance to identify the mechanism underlying tumor the Warburg effect to develop effective therapeutic strategies for GC.

In the present study, we report a novel circRNA, circCUL3 (circBase ID: hsa_circ_0008309, 312 bp), in GC using circRNA

Received 30 June 2020; accepted 20 August 2020;
https://doi.org/10.1016/j.omtn.2020.08.023.

[5]These authors contributed equally to this work.

Correspondence: Jun Zhao, Department of Gastrointestinal Surgery, Yijishan Hospital of Wannan Medical College, Wuhu, Anhui 241001, China.
E-mail: zhaojun.wnmc.edu@aliyun.com
Correspondence: Haitang Xie, Department of Drug Clinical Evaluation Center, Yijishan Hospital of Wannan Medical College, Wuhu, Anhui 241001, China.
E-mail: xiehaitang@sina.com

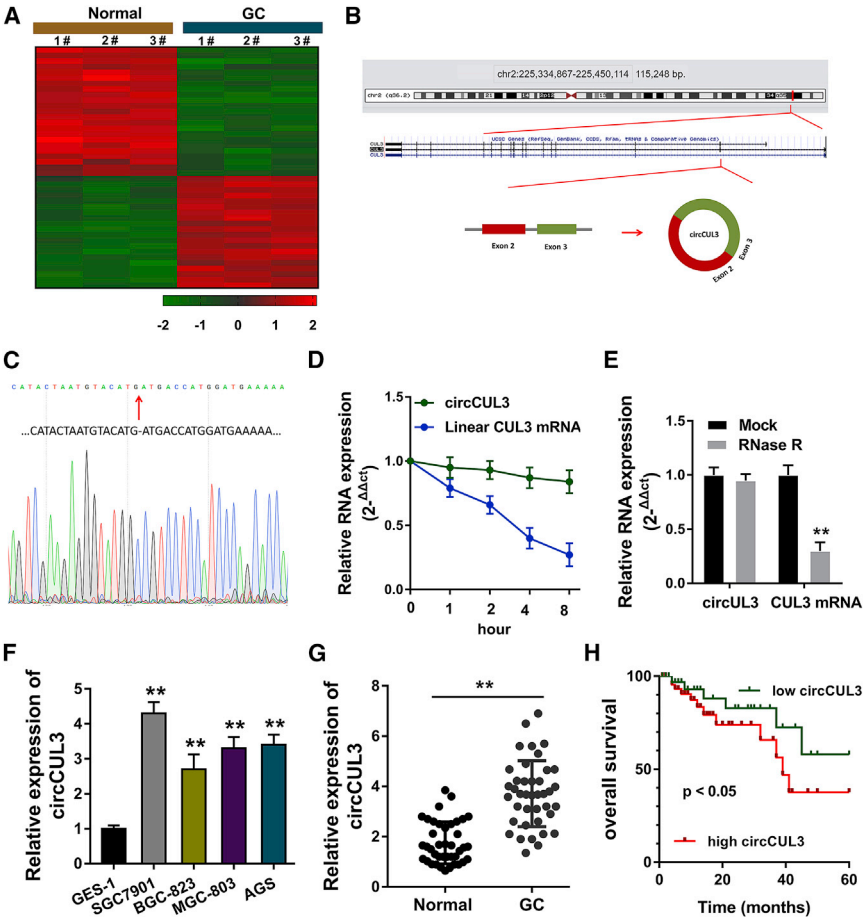

Figure 1. circCUL3 Is Highly Expressed in GC Tissues and Correlated with Unfavorable Prognosis

(A) circRNA microarray analysis was performed to screen the circRNA expression profile as compared to the normal tissue. (B) Schematic diagram demonstrates the identification of the circular structure for circCUL3. (C) Sanger sequencing determined the genomic size and sequence of circCUL3 as reported in the circBase database (http://www.circbase.org/). (D and E) (D) qRT-PCR showed the expression level of back-spliced circCUL3 or canonical linear CUL3 mRNA treated with RNase R administration and (E) actinomycin D. (F) qRT-PCR showed the circCUL3 expression level in GC cell lines and normal cells. (G) qRT-PCR showed the circCUL3 expression level in GC tissue specimens and normal specimens. (H) Survival analysis by Kaplan-Meier survival curves showed the survival rate for GC patients with high or low circCUL3 expression. Data are shown as mean ± SD. **p < 0.01.

microarray analysis and qRT-PCR validation. Results illustrated that circCUL3 was significantly upregulated in GC tissue and cells. Overexpression of circCUL3 was associated with poor prognosis in GC patients. Mechanistically, circCUL3 promoted the GC Warburg effect and progression through the circCUL3/miR-515-5p/signal transducer and activator of transcription (STAT)3/hexokinase 2 (HK2) axis. These findings provide mechanistic insights into the GC Warburg effect and bring a novel insight for understanding GC pathogenesis.

RESULTS

circCUL3 Is Highly Expressed in GC Tissues and Correlated with Unfavorable Prognosis

In order to discover the dysregulated circRNA in GC, a circRNA microarray analysis was performed to screen the circRNA expression profile as compared to the normal tissue (Figure 1A). circCUL3 is a 312-bp-long circRNA generated from the CUL3 gene exon 3 to exon 2 (Figure 1B). Subsequently, the head-to-tail splicing of circCUL3 was confirmed by Sanger sequencing. The genomic size was also determined as reported in the circBase database (Figure 1C). Then, qRT-PCR was performed to detect the expression level of back-spliced or canonical linear forms of CUL3 with or without RNase R administration (Figure 1D) and actinomycin D (Figure 1E). Data showed that the head-to-tail splicing form of circCUL3 was more stable than the linear mRNA. In GC cell lines, qRT-PCR demonstrated that circCUL3 expression was upregulated as compared to normal cells (Figure 1F). In GC tissue specimens, qRT-PCR demonstrated that circCUL3 expression was highly expressed as compared to normal tissue (Figure 1G). Survival analysis by Kaplan-Meier survival curves revealed that GC patients with high circCUL3 expression had lower survival rates (Figure 1H). In general, circCUL3 was identified to be highly expressed in GC tissues and correlated with unfavorable prognosis.

circCUL3 Promotes GC Cell Proliferation *In Vitro*, and Knockdown of circCUL3 Inhibits the Tumor Growth *In Vivo*

For the functional experiments of circCUL3, the knockdown and overexpression of circCUL3 were constructed, respectively, in SGC-7901 and BGC-823 cells (Figure 2A). A Cell Counting Kit-8 (CCK-8) proliferative assay demonstrated that the knockdown of circCUL3 repressed the proliferation of GC cells and that circCUL3 overexpression accelerated it (Figure 2B). An ethynyl deoxyuridine (EdU) assay illustrated that the knockdown of circCUL3 repressed the EdU-positive cells and that circCUL3 overexpression promoted the EdU-positive cells rate (Figure 2C). An *in vivo* heterograft mice assay illustrated that the knockdown of circCUL3 repressed tumor growth (neoplasm weight and volume) in mice injected with SGC-7901 cells that were transfected with short hairpin (shRNA) targeting circCUL3 (sh-circCUL3) (Figures 2D and 2E). In general, data suggest that circCUL3 promotes GC cell proliferation *in vitro* and that knockdown of circCUL3 inhibits tumor growth *in vivo*.

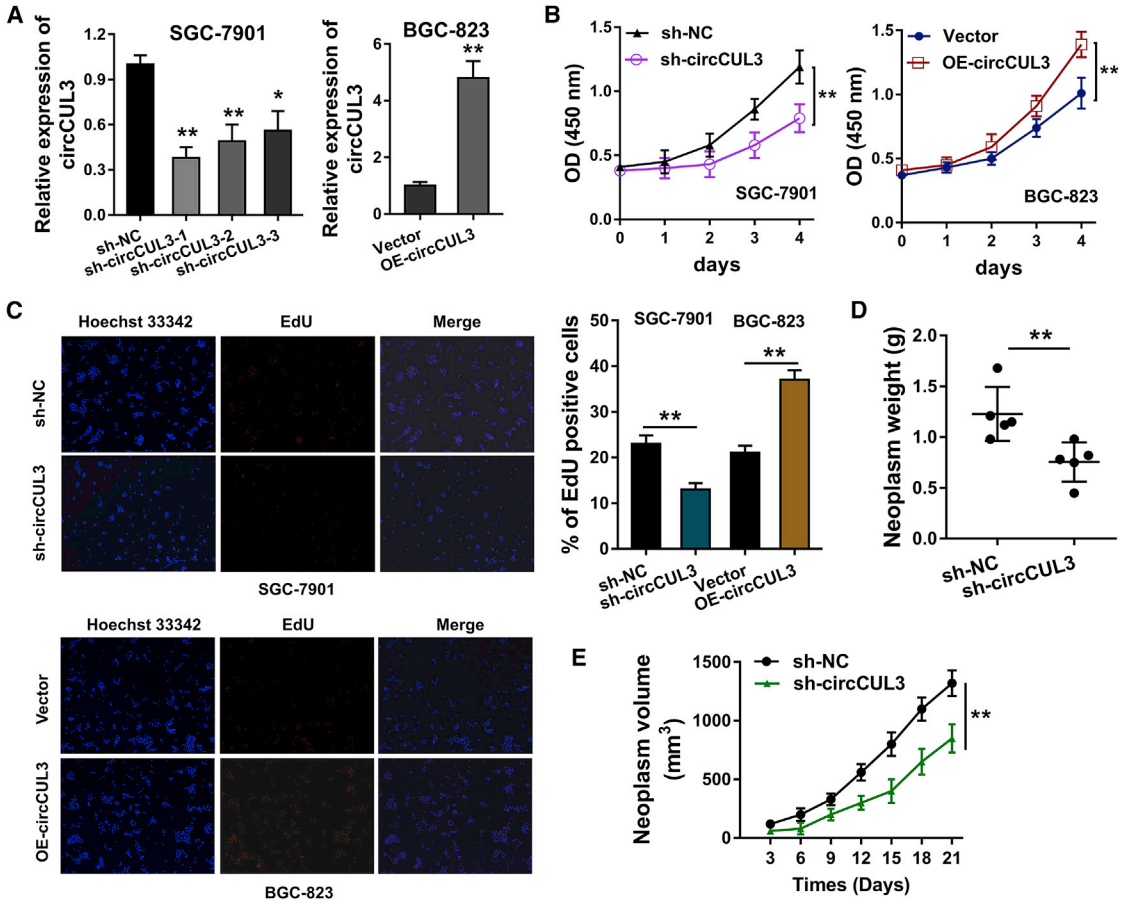

Figure 2. circCUL3 Promotes GC Cell Proliferation *In Vitro*, and Knockdown of circCUL3 Inhibits Tumor Growth *In Vivo*

(A) The knockdown and overexpression of circCUL3 were constructed respectively in SGC-7901 and BGC-823 cells. qRT-PCR was performed to detect circCUL3 expression. (B) A CCK-8 proliferative assay was performed to demonstrate the proliferation of GC cells transfected with sh-circCUL3 and circCUL3 overexpression (OE-circCUL3). (C) An EdU assay was performed to illustrate the proliferation (EdU-positive cells) of GC cells transfected with sh-circCUL3 and OE-circCUL3. (D and E) Neoplasm weight (D) and volume (E) were detected by an *in vivo* heterograft mice assay. The mice were injected with SGC-7901 cells that transfected with sh-circCUL3. Data are shown as mean ± SD. *$p < 0.05$, **$p < 0.01$.

circCUL3 Promotes the GC Cell Warburg Effect

To identify the role of circCUL3 on the GC cell Warburg effect, glucose consumption and lactate production were detected, and ATP quantity was determined. Results showed that circCUL3 knockdown reduced glucose consumption (Figure 3A), lactate production (Figure 3B), and ATP quantity (Figure 3C). In addition, circCUL3 overexpression (OE-circCUL3) promoted glucose consumption, lactate production, and ATP quantity. Extracellular acidification rate (ECAR) analysis for lactate-induced acidification of the medium surrounding cells showed that circCUL3 knockdown repressed the extracellular acidification rate and that circCUL3 overexpression promoted it (Figure 3D). Oxygen consumption rate (OCR) analysis for mitochondrial respiratory capacity showed that circCUL3 knockdown increased the OCR relative to the control group and that circCUL3 overexpression reduced it (Figure 3E). In general, data suggest that circCUL3 promotes the GC cell Warburg effect.

circCUL3 Targets miR-515-5p/STAT3 in GC Cells

In GC cell lines (SGC-7901, BGC-823), subcellular analysis demonstrated that circCUL3 was primarily located in the cytoplasmic portion, suggesting potential post-transcriptional regulation (Figure 4A). Online bioinformatics tools (TargetScan, RegRNA, CircNet) found that several microRNAs (miRNAs) might effectively interact with circCUL3, including miR-515-5p (Figure 4B). Subsequently, the wild-type (WT) and corresponding mutant (Mut) were constructed targeting miR-515-5p in GC cells. Moreover, a luciferase reporter assay illustrated that circCUL3 WT closely correlated with miR-515-5p (Figure 4C). The subcellular location analysis was measured using RNA-fluorescence *in situ* hybridization (FISH), and results demonstrated that circCUL3 and miR-515-5p were both mainly distributed in cytoplasm (Figure 4D). Moreover, online bioinformatics tools (StarBase, http://starbase.sysu.edu.cn/) found that miR-515-5p targets the 3′ UTR of HK2 mRNA (Figure 4E). qRT-PCR analysis showed that

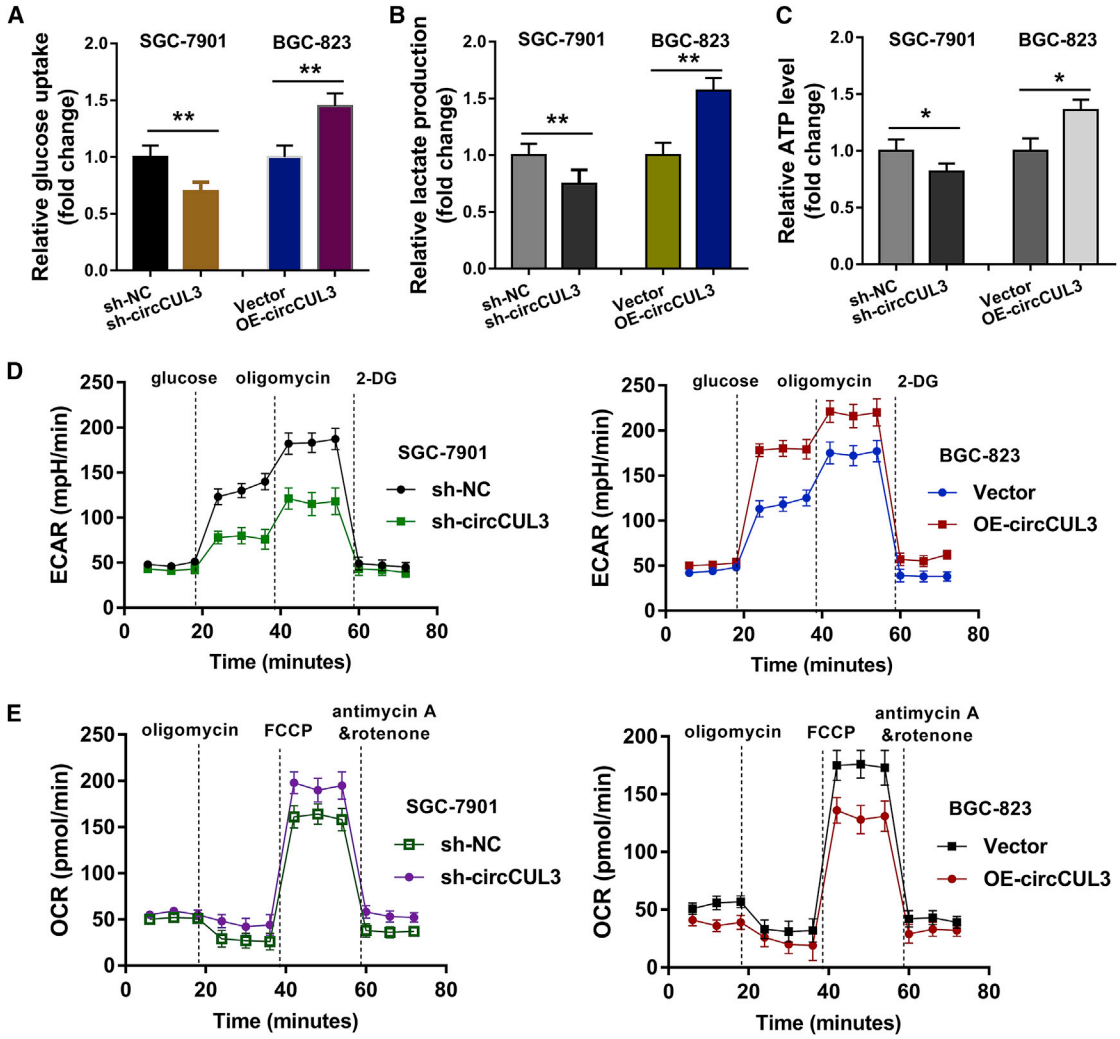

Figure 3. circCUL3 Promotes the GC Cell Warburg Effect

(A) Glucose consumption analysis revealed the glucose consumption in SGC-7901 and BGC-823 cells transfected with circCUL3 knockdown or OE-circCUL3. (B) Lactate production analysis revealed the lactate production in SGC-7901 and BGC-823 cells transfected with circCUL3 knockdown or OE-circCUL3. (C) ATP quantity analysis revealed the ATP quantity in SGC-7901 and BGC-823 cells transfected with circCUL3 knockdown or OE-circCUL3. (D) ECAR analysis for lactate-induced acidification of the medium surrounding cells was performed. (E) OCR analysis for mitochondrial respiratory capacity was conducted using a Seahorse XFp assay. Data are shown as mean ± SD. *$p < 0.05$, **$p < 0.01$.

circCUL3 overexpression enforced the STAT3 mRNA, while miR-515-5p mimics reduced the STAT3 mRNA expression. In addition, the co-transfection of circCUL3 overexpression and miR-515-5p mimics rescued the STAT3 mRNA expression (Figure 4F). In conclusion, these finding indicate that circCUL3 targets miR-515-5p/STAT3 in GC cells.

Transcription Factor STAT3 Activates the Expression of HK2

Given that STAT3 is a critical transcription factor in GC, we presumed that STAT3 might play a role on the Warburg effect. Online bioinformatics predictive tools (JASPAR, http://jaspar.genereg.net/) hinted that transcription factor STAT3 could target the promoter region of the HK2 gene (Figure 5A). The binding relationship between STAT3 and the HK2 promoter was detected using a chromatin immunoprecipitation (ChIP) assay, showing the molecular interaction within STAT3 and HK2 (Figure 5B). A luciferase reporter assay demonstrated the luciferase activity of the HK2 promoter, and data showed that STAT3 promoted the promoter luciferase activity of the WT sequence (Figure 5C). STAT3 overexpression plasmids were transfected into SGC-7901 cells to enhance STAT3 expression. Moreover, the overexpression of STAT3 also upregulated the HK2 protein level (Figure 5D). In SGC-7901 and BGC-823 cells, qRT-PCR revealed that HK2 mRNA levels were upregulated in the STAT3 overexpression transfection (Figure 5E). Pearson correlation analysis of STAT3 and HK2 detection in the GC tissues cohort suggested the positive relationship of STAT3 and HK2 (Figure 5F). In conclusion, these findings imply that transcription factor STAT3 activates the expression of HK2 in GC.

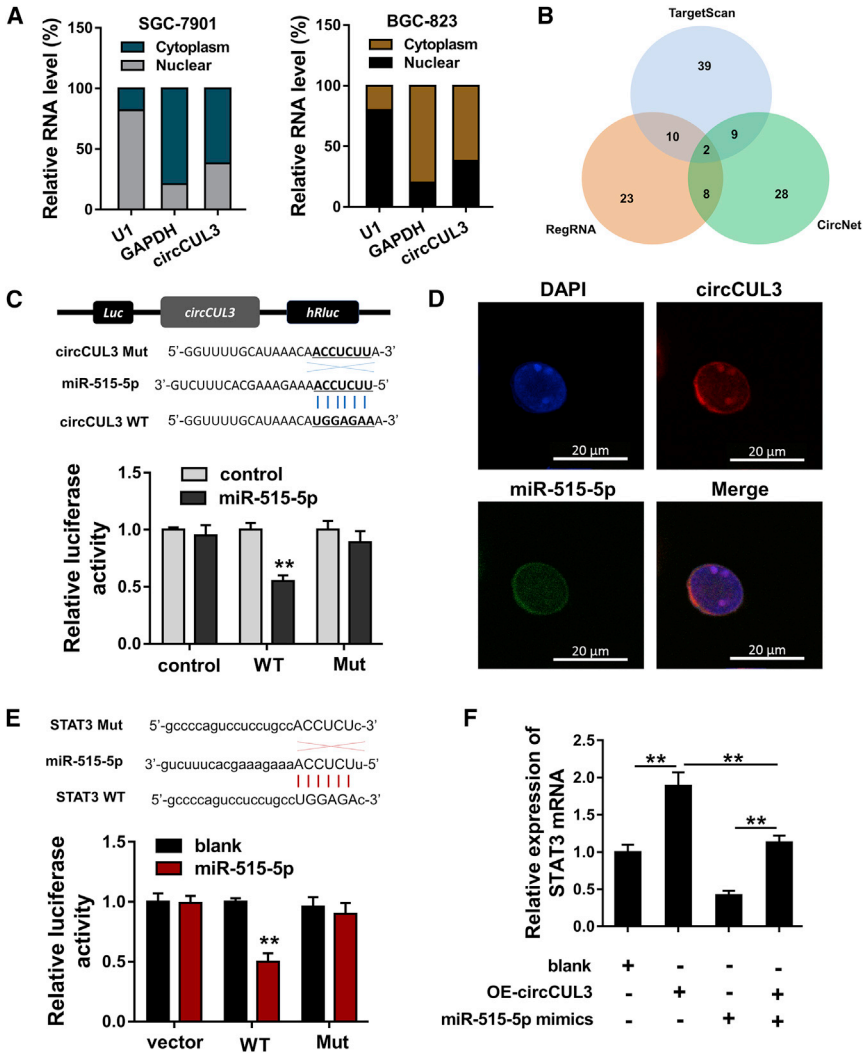

Figure 4. circCUL3 Targets miR-515-5p/STAT3 in GC Cells

(A) Subcellular analysis demonstrated the circCUL3 location in the cytoplasm or nuclear material in GC cell lines (SGC-7901, BGC-823). (B) Online bioinformatics tools (TargetScan, RegRNA, CircNet) found that several miRNAs might effectively interact with circCUL3, including miR-515-5p. (C) The wild-type (WT) and corresponding mutant (Mut) of circCUL3 were constructed targeting miR-515-5p. A luciferase reporter assay illustrated the correlation within circCUL3 WT and miR-515-5p. (D) RNA-FISH demonstrated the distribution of circCUL3 and miR-515-5p in cytoplasm and nuclear material. (E) The WT and corresponding Mut of the STAT3 mRNA 3′ UTR were constructed targeting miR-515-5p. A luciferase reporter assay illustrated the correlation within STAT3 mRNA WT and miR-515-5p. (F) qRT-PCR analysis showed the STAT3 mRNA in BGC-823 cells transfected with circCUL3 overexpression and or miR-515-5p mimics. Data are shown as mean ± SD. $^{**}p < 0.01$.

DISCUSSION

With the tremendous advancement of high-throughput sequencing technology, great numbers of noncoding RNAs have been identified in human cancer.[20–22] In addition, bioinformatics tools bring greater analytical capability to process the microarray data and unlock a potential regulator for cancers. For GC tumorigenesis, numerous circRNAs have been identified to participate in the pathophysiological process and regulate different tumorigenic phenotypes.

The Warburg effect is a significant hallmark in GC tumorigenesis.[23] More and more evidence emphasizes the crucial role of circRNAs in the GC Warburg effect. In the present study, microarray analysis results revealed the numerous dysregulated circRNAs in the GC tissue. Herein, we report a novel circRNA, circCUL3 (circBase ID: hsa_circ_0008309, 312 bp), which was upregulated in the GC tissue as compared to the normal adjacent samples. The overexpression of circCUL3 was closely correlated with the poor prognosis of GC patients, indicating the risk factor of circCUL3 for the GC population. In the cellular functions, gain- and loss-of-function assay results found that circCUL3 promoted the proliferation of GC cells. Therefore, these findings indicated that circCUL3 might function as an oncogenic factor for GC.

As this circRNA research has proceeded, the functions and mechanism of circRNAs in GC have been extensively investigated.[24] The regulation range of circRNAs relates to tumor cell differentiation, invasiveness, metastasis, chemotherapy resistance, and stemness characteristics.[25] For instance, circRNA circCYFIP2 (hsa_circ_0003506, 366 nt) was spliced from the CYFIP2 gene. circCYFIP2 was found to be significantly upregulated in GC tissues, and the high expression was associated with metastasis and poor prognosis of GC patients.[26] Moreover, the evident downregulation of circCCDC9 was closely correlated with tumor size, lymph node invasion, advanced clinical stage, and overall survival in GC patients. Overexpression of circCCDC9 significantly inhibited the migration, proliferation, and invasion of GC cells *in vitro* and tumor growth and metastasis *in vivo* through acting as a competing endogenous RNA (ceRNA) of miR-6792-3p to relieve CAV1 expression.[1] A novel circRNA named circMRPS35 was screened out by RNA sequencing (RNA-seq) in GC tissues, which recruits histone acetyltransferase KAT7 to the promoters of FOXO1 and FOXO3a genes through acting as a modular scaffold.[27] Overall, these findings support the conclusion that circRNAs momentously regulate the tumorigenesis of GC.

In the present study, our results indicated that circCUL3 might serve as a ceRNA of miR-515-5p. Mechanistically, STAT3 acted as a target of miR-515-5p, and then transcription factor STAT3 combines with the promotor region of HK2. Overall, we draw a conclusion from these

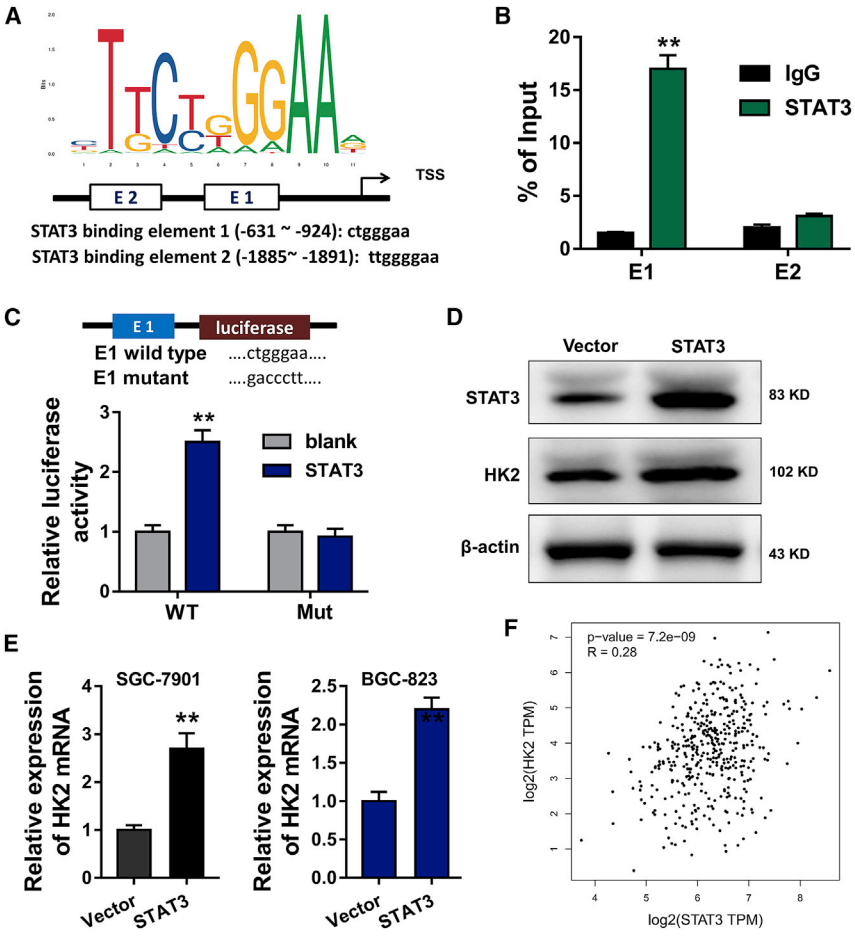

Figure 5. Transcription Factor STAT3 Activates the Expression of HK2

(A) An online bioinformatics predictive tool (JASPAR, http://jaspar.genereg.net/) hinted that transcription factor STAT3 could target the promoter region of the HK2 gene. (B) A ChIP assay was performed to identify the binding relationship between STAT3 and the HK2 promoter. (C) Mut and WT sequences of the HK2 first element were respectively constructed. A luciferase reporter assay was performed to detect the luciferase activity. (D) STAT3 overexpression plasmids were transfected into SGC-7901 cells. A western blot assay was performed to detect the STAT3 and HK2 protein expression. (E) qRT-PCR was performed to detect the HK2 mRNA expression in SGC-7901 and BGC-823 cells. (F) Pearson correlation analysis of STAT3 and HK2 was detected in the GC tissues cohort. Data are shown as mean ± SD. **$p < 0.01$.

data that circCUL3/miR-515-5p/STAT3/HK2 axis in the GC aerobic glycolysis progression (Warburg effect). HK2 is a critical element in the Warburg effect and participates in aerobic glycolysis progression. For example, in GC, miR-181b targets HK2 to repress HK2 expression, thereby reducing glucose uptake and lactate production.[28]

In summary, the present research findings revealed a novel circRNA, circCUL3 (hsa_circ_0008309, 312 bp), using microarray analysis. circCUL3 was upregulated in GC tissues, and the overexpression of circCUL3 was correlated with an unfavorable prognosis of GC patients. Enhanced circCUL3 expression promoted the Warburg effect and tumor formation of GC. Moreover, these results make to a conclusion from the data that circCUL3/miR-515-5p/STAT3/HK2 axis in the GC aerobic glycolysis progression (Warburg effect) (Figure 6). Therefore, the data indicate a novel function of circCUL3 in reprogramming the GC metabolic process, which provides a potential therapeutic target for the GC treatment.

MATERIALS AND METHODS

Patients and Specimens

All GC samples and matched normal tissue (40 pairs) used in this study were from patients enrolled at the Yijishan Hospital of Wannan Medical College. This study had been approved by the Ethics Committee of the Yijishan Hospital of Wannan Medical College. Informed consent, agreement, and ethical regulations of patients have been obtained. Tumor stage was defined according to the criteria of the tumor, node, and metastasis (TNM) classification of the International Union against Cancer (Table 1).

Cell Culture

Human GC cell lines (SGC-7901, BGC-823, MGC-803, AGS) as well as their control normal cell line (GES-1) were provided by the Cell Bank of the Chinese Academy of Sciences (Shanghai, China) and American Type Culture Collection (ATCC, Manassas, VA, USA). Cell culture was performed in compliance with ATCC protocols and incubated in a 5% CO_2 atmosphere at 37°C.

Transfection

Specifically synthesized sh-circCUL3 1/2/3 and the nonspecific shRNA as a negative control (sh-NC) for lentiviral vectors were provided by GenePharma (Shanghai, China). circCUL3 cDNA was amplified and then inserted into the coding sequence (CDS) into the p3 × FLAGCMV-10 vector (Sigma-Aldrich, St. Louis, MO, USA) to construct circCUL3 overexpression. miRNA mimic and inhibitor were purchased from RiboBio (Guangzhou, China). GC cells were transfected individually with these plasmids via Lipofectamine 3000 (Invitrogen, Carlsbad, CA, USA). After 48 h, the stably transfected cells were selected out using 2 μg/mL puromycin treatment.

qRT-PCR

GC cells were re-suspended in 1 mL of TRIzol (Invitrogen) and total RNA was extracted from the cells and then reverse transcribed as described before.[29] Total cellular RNA was reverse transcribed

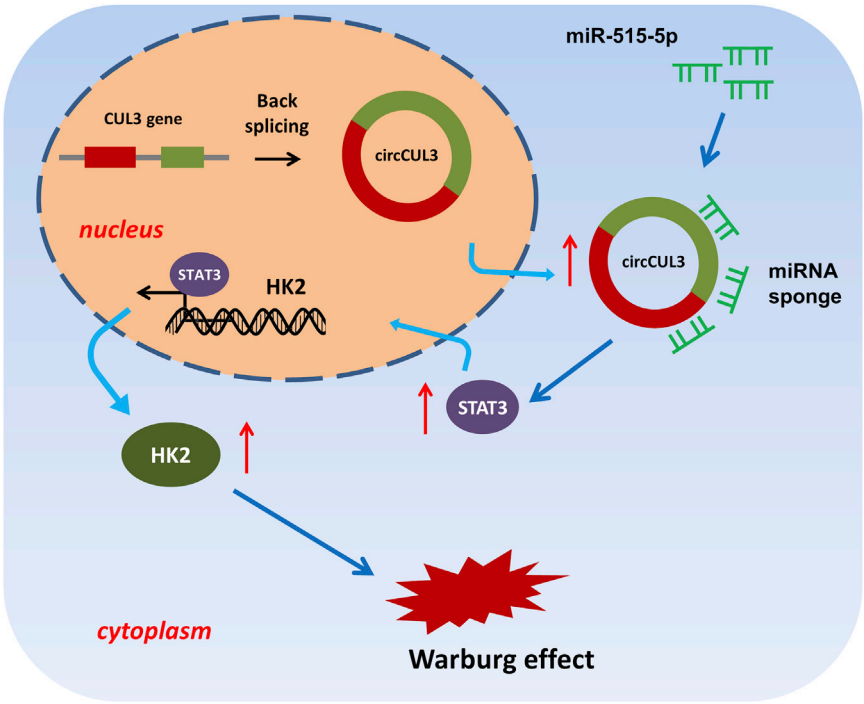

Figure 6. Circular RNA circCUL3 Accelerates the GC Warburg Effect through the miR-515-5p/STAT3/HK2 Axis

into cDNA. For circRNA and mRNA, cDNA was synthesized using a HiScript II first-strand cDNA synthesis kit (Vazyme, Nanjing, China). For miRNA, cDNA was synthesized by an All-in-One miRNA first-strand cDNA synthesis kit (GeneCopoeia, Rockville, MD, USA). Gene expression was detected by real-time PCR analyses for circRNA, miRNA, or mRNA on a 7500 real-time PCR system (Applied Biosystems) as previously described. β-Actin and U6 served as internal controls. All primers used in this study are listed in Table S1.

RNase R and Actinomycin D Treatment

In order to detect circRNA stability, RNase R and actinomycin D treatment assays were performed. First, for the RNase R assay, 2 μg of total RNA was incubated with or without RNase R (3 U/μg, Geneseed Biotech, Guangzhou, China) for 10 min at 37°C. Then, RNA was purified using RNeasy MinElute Cleanup kit (Qiagen, Hilden, Germany). For actinomycin D treatment, DMSO (negative control) or 2 mg/mL actinomycin D (Sigma-Aldrich, St. Louis, MO, USA) was administrated. The RNA expression levels were analyzed by qRT-PCR.

Western Blotting Analysis

GC cells were lysed for protein lysis on ice using radioimmunoprecipitation assay (RIPA) lysis buffer (Dalian Meilun Biotechnology, China) containing protease inhibitor cocktails (Fudebio, Hangzhou, China). Total protein from each sample was separated by SDS-PAGE gels and transferred onto polyvinylidene fluoride (PVDF, 0.22-μm) membranes (Amersham Bioscience, Piscataway, NJ, USA). Subsequently, the PVDF membranes were blocked with skim milk powder (5%) in Tris-buffered saline with Tween 20 (TBST) at room temperature and incubated with primary antibodies (anti-STAT3, anti-HK2, Abcam, 1:1,000) overnight at 4°C. Then, the membranes were washed with TBST and incubated by horseradish peroxidase (HRP)-conjugated secondary antibody (anti-ACTINB). Quantitative analysis of band intensity was determined using ImageJ software.

Proliferation Assay

Cellular proliferation ability was detected using a CCK-8 assay and EdU incorporation assay. For CCK-8, a total of approximately 2×10^3 cells/well were seeded in 96-well plates. After culturing at the indicated times (24, 48, 72, and 96 h), the cellular viability was detected using a CellTiter-Glo luminescent cell viability assay (Promega, Madison, WI, U.S.A.) according to the manufacturer's instructions. For the EdU incorporation assay, EdU (10 mM) was added to each well and cells were fixed with 4% formaldehyde for 30 min. After washing, EdU was detected with a Click-iT EdU kit, and images were visualized using a fluorescence microscope (Olympus).

Glucose Consumption, Lactate Production, and ATP Level Measurement

Briefly, the experimental methods for glucose consumption, lactate production, and ATP level measurement were as previously described.[30] Glucose was determined by a glucose assay kit (Sigma, St. Louis, MO, USA). Lactate levels were measured by a lactate colorimetric/fluorometric assay kit (BioVision, Mountain View, CA, USA). ATP level was determined using an ATP determination kit (Thermo Fisher Scientific, Waltham, MA, USA).

ECAR and OCR

ECAR and OCR were determined using a Seahorse XFe96 analyzer (Seahorse Bioscience, Agilent Technologies). The stable transfected cells (1×10^4 cells/well) were seeded into 96-well XF cell culture microplates. After 24 h, the medium was replaced by XF base medium (pH 7.4) containing glucose (10 mM), glutamine (1 mM), 2-deoxyglucose (2-DG) (50 mM), and oligomycin (1 μM). Finally, the ECAR was detected using an XFe96 analyzer (Seahorse Bioscience). For the OCR, cells were respectively treated with oligomycin (1 mM), carbonyl cyanide 4-(trifluoromethoxy)phenylhydrazone (FCCP), and antimycin A (2 mM) and rotenone. The data of ECAR and OCR were measured and normalized to total protein content (milli-pH [mpH]/min).

Table 1. Relationship between circCUL3 and the Clinicopathological Characteristic of GC Patients

			circCUL3		
			Low	High	p Value
Age	<60	18	8	10	0.487
	≥60	22	10	12	
Sex	male	27	14	13	0.185
	female	13	4	9	
Tumor size	<3.5 cm	23	8	15	0.023*
	≥3.5 cm	17	10	7	
Histological grade	well/moderate	14	8	6	0.216
	poor/other	26	10	16	
T stage	T1–T2	16	8	8	0.009*
	T3–T4	24	10	14	
TNM stage	I–II	18	10	8	0.178
	III–IV	22	8	14	
Lymphatic metastasis	present	19	7	12	0.652
	absent	21	11	10	

Well, well-differentiated adenocarcinoma; moderate, moderately differentiated adenocarcinoma; poor, poorly differentiated adenocarcinoma; other, other histological type; TNM, tumor-node-metastasis. *Represents statistical difference ($p < 0.05$).

Subcellular Location Analysis

RNA was isolated from nuclear and cytoplasmic fractions using a Paris kit (Invitrogen, Carlsbad, CA, USA) following the manufacturer's protocol. The RNA of nuclear and cytoplasmic fractions was eluted and then detected using qRT-PCR. For FISH, Cy3-labeled circCUL3 probes and 6-carboxyfluorescein FAM-labeled miR-515-5p probes were synthesized by GenePharma (Shanghai, China). FISH was performed using a FISH kit (GenePharma) according to the manufacturer's instructions. Nuclei were stained by DAPI. Analysis was performed using Image-Pro Plus 6.0 (Media Cybernetics, Rockville, MD, USA) software.

Luciferase Reporter Assay

The reporter plasmids (pGL3-firefly or Renilla luciferase) containing the circCUL3 sequence, STAT3 3′ UTR, and the HK2 promoter region, as well as matched Mut sequences, were designed by GeneChem (Shanghai, China). 293T cells were co-transfected with these plasmids and miR-515-5p mimic or negative control (RiboBio, Guangzhou, China). Firefly luciferase activity was calculated and normalized to Renilla luciferase activity. Luciferase activities were detected using a multimode detector (Promega).

ChIP Assay

A ChIP assay was performed using a Magna ChIP kit (Millipore, Billerica, MA, USA) according to the manufacturer's manual. Briefly, 1×10^7 SGC-7901 cells were fixed with formaldehyde (1%, Sigma) and the nuclear isolation was extracted. Then, the isolation was purified and sonicated into fragments (200–1,000 bp) and immunoprecipitated with anti-STAT3 antibody (Abcam, ab32500, 1:1,000) or anti-immunoglobulin G (IgG). The putative transcriptional binding sites were predicted by JASPAR (http://jaspar.genereg.net/). The immunoprecipitated complex was collected and the reverse transcription was detected by real-time PCR normalized to input control.

In Vivo Xenograft Assay

Animal studies were approved by the Laboratory Animal Welfare and Ethics Committee of the Yijishan Hospital of Wannan Medical College. For the *in vivo* tumor study, male BALB/c mice (6 weeks old, 15–20 g weight) were provided from the SLAC Laboratory Animal Center (Shanghai, China). SGC-7901 cell lines were stably transfected with sh-circCUL3 and then subcutaneously injected into BALB/c mice. Every 3 days, tumor size (volume) was detected by caliper and calculated using the following equation: (longer axes × shorter axes × shorter axes)/2. Tumor weight was calculated after excision.

Statistical Analyses

Statistical analyses were performed with SPSS 19.0 software (Abbott Laboratories, Chicago, IL, USA) and GraphPad Prism 7.0 (GraphPad, La Jolla, CA, USA). All data were analyzed with an unpaired Student's t test or one-way ANOVA plus and expressed as mean ± standard deviation (SD). Survival analysis was performed using the Kaplan-Meier method and log-rank test for survival curves. Univariate and multivariate analyses were performed using the Cox regression model. p values less than 0.05 were considered statistically significant.

SUPPLEMENTAL INFORMATION

Supplemental Information can be found online at https://doi.org/10.1016/j.omtn.2020.08.023.

AUTHOR CONTRIBUTIONS

Z.P., M.X., and X.Y. performed the work and the statistical analyses. H.X. and J.Z. were responsible for the funding and revision of the manuscript.

CONFLICTS OF INTEREST

The authors declare no competing interests.

ACKNOWLEDGMENTS

This work was supported by the National Natural Science Foundation of China (81173134); the Natural Science Research Project of Anhui University (KJ2017A248); the Nature Science Research Project of Anhui Province (1808085MH271); the Talent Introduction Program of Yijishan Hospital of Wannan Medical College (YR202005); the Science and Technology Innovation Team of Yijishan Hospital of Wannan Medical College (YPF2019016); and the Talent introduction project of Yijishan Hospital of Wannan Medical College (YR202005).

REFERENCES

1. Bonelli, P., Borrelli, A., Tuccillo, F.M., Silvestro, L., Palaia, R., and Buonaguro, F.M. (2019). Precision medicine in gastric cancer. World J. Gastrointest. Oncol. *11*, 804–829.

2. Gao, Y., Xi, H., Wei, B., Cui, J., Zhang, K., Li, H., Cai, A., Shen, W., Li, J., Rosell, R., et al. (2019). Association between liquid biopsy and prognosis of gastric cancer patients: a systematic review and meta-analysis. Front. Oncol. *9*, 1222.

3. Jones, J.O., and Smyth, E.C. (2020). Gastroesophageal cancer: navigating the immune and genetic terrain to improve clinical outcomes. Cancer Treat. Rev. *84*, 101950.
4. Zheng, L.N., Wen, F., Xu, P., and Zhang, S. (2019). Prognostic significance of malignant ascites in gastric cancer patients with peritoneal metastasis: a systemic review and meta-analysis. World J. Clin. Cases *7*, 3247–3258.
5. Symeonidis, D., Diamantis, A., Bompou, E., and Tepetes, K. (2019). Current role of lymphadenectomy in gastric cancer surgery. J. BUON *24*, 1761–1767.
6. Wang, Q., Liu, G., and Hu, C. (2019). Molecular classification of gastric adenocarcinoma. Gastroenterol. Res. *12*, 275–282.
7. Fang, X., Wen, J., Sun, M., Yuan, Y., and Xu, Q. (2019). circRNAs and its relationship with gastric cancer. J. Cancer *10*, 6105–6113.
8. Tang, X., Zhu, J., Liu, Y., Chen, C., Liu, T., and Liu, J. (2019). Current understanding of circular RNAs in gastric cancer. Cancer Manag. Res. *11*, 10509–10521.
9. Yang, J., Liu, J., Zhao, S., and Tian, F. (2020). N^6-methyladenosine METTL3 modulates the proliferation and apoptosis of lens epithelial cells in diabetic cataract. Mol. Ther. Nucleic Acids *20*, 111–116.
10. Belousova, E.A., Filipenko, M.L., and Kushlinskii, N.E. (2018). Circular RNA: new regulatory molecules. Bull. Exp. Biol. Med. *164*, 803–815.
11. Pervouchine, D.D. (2019). Circular exonic RNAs: when RNA structure meets topology. Biochim. Biophys. Acta. Gene Regul. Mech. *1862*, 194384.
12. Chen, Y., Lin, Y., Shu, Y., He, J., and Gao, W. (2020). Interaction between N^6-methyladenosine (m^6A) modification and noncoding RNAs in cancer. Mol. Cancer *19*, 94.
13. Zhang, L., Hou, C., Chen, C., Guo, Y., Yuan, W., Yin, D., Liu, J., and Sun, Z. (2020). The role of N^6-methyladenosine (m^6A) modification in the regulation of circRNAs. Mol. Cancer *19*, 105.
14. Luo, Z., Rong, Z., Zhang, J., Zhu, Z., Yu, Z., Li, T., Fu, Z., Qiu, Z., and Huang, C. (2020). Circular RNA circCCDC9 acts as a miR-6792-3p sponge to suppress the progression of gastric cancer through regulating CAV1 expression. Mol. Cancer *19*, 86.
15. Lonetto, G., Koifman, G., Silberman, A., Attery, A., Solomon, H., Levin-Zaidman, S., et al. (2019). Mutant p53-dependent mitochondrial metabolic alterations in a mesenchymal stem cell-based model of progressive malignancy. Cell Death Differ *26*, 1566–1581.
16. Lane, A.N., Higashi, R.M., and Fan, T.W. (2019). Metabolic reprogramming in tumors: contributions of the tumor microenvironment. Genes Dis. *7*, 185–198.
17. Jing, Y.Y., Cai, F.F., Zhang, L., Han, J., Yang, L., Tang, F., Li, Y.B., Chang, J.F., Sun, F., Yang, X.M., et al. (2020). Epigenetic regulation of the Warburg effect by H2B monoubiquitination. Cell Death Differ. *27*, 1660–1676.
18. Vanhove, K., Graulus, G.J., Mesotten, L., Thomeer, M., Derveaux, E., Noben, J.P., Guedens, W., and Adriaensens, P. (2019). The metabolic landscape of lung cancer: new insights in a disturbed glucose metabolism. Front. Oncol. *9*, 1215.
19. Zhang, X., Wang, S., Wang, H., Cao, J., Huang, X., Chen, Z., Xu, P., Sun, G., Xu, J., Lv, J., and Xu, Z. (2019). Circular RNA circNRIP1 acts as a microRNA-149-5p sponge to promote gastric cancer progression via the AKT1/mTOR pathway. Mol. Cancer *18*, 20.
20. Chen, T., and Tyagi, S. (2020). Integrative computational epigenomics to build data-driven gene regulation hypotheses. Gigascience *9*, giaa064.
21. Ver Donck, F., Downes, K., and Freson, K. (2020). Strengths and limitations of high-throughput sequencing for the diagnosis of inherited bleeding and platelet disorders. J. Thromb. Haemost. *18*, 1839–1845.
22. Huang, W., Yang, Y., Wu, J., Niu, Y., Yao, Y., Zhang, J., et al. (2020). Circular RNA cESRP1 sensitises small cell lung cancer cells to chemotherapy by sponging miR-93-5p to inhibit TGF-β signalling. Cell Death Differ. *27*, 1709–1727.
23. Regdon, Z., Robaszkiewicz, A., Kovács, K., Rygielska, Ż., Hegedűs, C., Bodoor, K., Szabó, É., and Virág, L. (2019). LPS protects macrophages from AIF-independent parthanatos by downregulation of PARP1 expression, induction of SOD2 expression, and a metabolic shift to aerobic glycolysis. Free Radic. Biol. Med. *131*, 184–196.
24. Ruan, Y., Li, Z., Shen, Y., Li, T., Zhang, H., and Guo, J. (2020). Functions of circular RNAs and their potential applications in gastric cancer. Expert Rev. Gastroenterol. Hepatol. *14*, 85–92.
25. Wei, L., Sun, J., Zhang, N., Zheng, Y., Wang, X., Lv, L., Liu, J., Xu, Y., Shen, Y., and Yang, M. (2020). Noncoding RNAs in gastric cancer: implications for drug resistance. Mol. Cancer *19*, 62.
26. Lin, J., Liao, S., Li, E., Liu, Z., Zheng, R., Wu, X., and Zeng, W. (2020). circCYFIP2 acts as a sponge of miR-1205 and affects the expression of its target gene E2F1 to regulate gastric cancer metastasis. Mol. Ther. Nucleic Acids *21*, 121–132.
27. Jie, M., Wu, Y., Gao, M., Li, X., Liu, C., Ouyang, Q., Tang, Q., Shan, C., Lv, Y., Zhang, K., et al. (2020). circMRPS35 suppresses gastric cancer progression via recruiting KAT7 to govern histone modification. Mol. Cancer *19*, 56.
28. Li, L.Q., Yang, Y., Chen, H., Zhang, L., Pan, D., and Xie, W.J. (2016). MicroRNA-181b inhibits glycolysis in gastric cancer cells via targeting hexokinase 2 gene. Cancer Biomark. *17*, 75–81.
29. Wang, H., Chen, W., Jin, M., Hou, L., Chen, X., Zhang, R., Zhang, J., and Zhu, J. (2018). circSLC3A2 functions as an oncogenic factor in hepatocellular carcinoma by sponging miR-490-3p and regulating PPM1F expression. Mol. Cancer *17*, 165.
30. Liao, M., Liao, W., Xu, N., Li, B., Liu, F., Zhang, S., Wang, Y., Wang, S., Zhu, Y., Chen, D., et al. (2019). lncRNA EPB41L4A-AS1 regulates glycolysis and glutaminolysis by mediating nucleolar translocation of HDAC2. EBioMedicine *41*, 200–213.